Journal of Alloys and Compounds 509 (2011) 10040–10049

Contents lists available at ScienceDirect

Journal of Alloys and Compounds

journal homepage: www.elsevier.com/locate/jallcom

Dielectric and tunability properties of La-doped $BaTiO_3$ ceramics

A. Ianculescu[a], Z.V. Mocanu[b], L.P. Curecheriu[b,*], L. Mitoseriu[b,*], L. Padurariu[b], R. Trușcă[c]

[a] Department of Oxide Materials Science and Engineering, "Politehnica" University of Bucharest, 1-7 Gh. Polizu, P.O. Box 12-134, 011061 Bucharest, Romania
[b] Department of Physics, "Alexandru Ioan Cuza" University, Bv. Carol 11, Iasi, 700506, Romania
[c] S.C. METAV–Research & Development Bucharest, 31 C. A. Rosetti, 020011 Bucharest, Romania

ARTICLE INFO

Article history:
Received 15 March 2011
Received in revised form 15 June 2011
Accepted 5 August 2011
Available online 12 August 2011

Keywords:
Insulator
Electrical properties
Ferroelectricity
Multipolarization mechanism

ABSTRACT

La-doped $BaTiO_3$ ($x = 0.001$; 0.0025; 0.005; 0.01; 0.025) ceramics were prepared via conventional solid state reaction and sintered at 1300 °C for 6 h, resulting in dense single phase ceramics with homogeneous microstructures. The temperature dependence of dielectric permittivity of the ceramics has been investigated. The results show a decrease of T_C with lanthanum addition. The degree of diffuseness of phase transition is more pronounced for high La content, implying the existence of a composition-induced phase transition of the ceramics. The dc-tunability at room temperature was investigated and experimental data were discussed in terms of the Johnson model completed with a Langevin term that describes "extrinsic" contribution to the non-linear $\varepsilon(E)$ dependences.

1. Introduction

Dielectric response in polar dielectrics with respect to the external electric field is an important issue in the dielectrics/ferroelectrics physics. In addition, a new type of electronic device making use of the variation of dielectric constant of polar dielectrics under dc electric fields has been developed extensively as next-generation radar and microwave communication devices [1–5]. For the microwave applications the most studied materials were (Ba,Sr)TiO_3 [6] and (Pb,Sr)TiO_3 [5] and most promising results were reported especially in (Ba,Sr)TiO_3 films [7]. In spite of intensive studies of tunability in various systems, it is important to design new materials which can respond to applications requirements (dielectric constant around 1000 and losses less than 0.03) [2]. In addition, there are some questions that still remain to be clarified, as for example the origin of tunability, the contributions to the dielectric constant and losses and the ways to control them. The origin of tunability was attributed to the rate of transformation of the non-ferroelectric state into a ferroelectric state under the applied electric field [8]. Starting from the Landau–Ginzburg–Devonshire's phenomenological theory, Johnson obtained a relationship between permittivity and the external electric field [9], by considering a non-linear polarization. According to this equation, the relaxors ferroelectrics should possess higher tunabilities because their zero-field permittivities are higher than those of classical ferroelectrics.

$BaTiO_3$-based solid solutions are environment-friendly ferroelectric relaxors with similar performances as many Pb-based electroceramic materials [10]. The design and exploration of Pb-free materials in new structures for tunable devices are of high interest, together with fundamental studies related to the origin of their dielectric non-linearity. According to these considerations La-doped $BaTiO_3$ (denoted as BLT) can be a promising candidate for tunable materials. Lanthanum has a fixed 3+ oxidation state and due to its ionic radius of 1.36 Å to be compared with 1.61 Å of Ba^{2+} and of 0.74 Å for Ti, it will only occupy A sites within the perovskite lattice. The charge balance compensation mechanism when Ba^{2+} is replaced by La^{3+} has long been a matter of debate. Undoped $BaTiO_3$ is a good insulator with a high energy gap $E_g = 3.5$ eV. When $BaTiO_3$ is doped with low amounts (<0.5 at.%) of higher valence foreign ions as La^{3+} on Ba^{2+} sites or Nb^{5+} and Sb^{5+} on Ti^{4+} sites, a semiconducting behaviour was commonly observed, indicating compensation via electronic "donor-doping" mechanism, or a polaronic mechanism involving the reduction of a small amount of Ti^{4+} ions to Ti^{3+} [11–16], according to the reactions (1) and (1′):

$$La_2O_3 + 2TiO_2 \rightleftarrows 2La_{Ba}^{\bullet} + 2Ti_{Ti}^{\times} + 6O_O^{\times} + \frac{1}{2}O_2(g) + 2e' \quad (1)$$

$$La_2O_3 + 2TiO_2 \rightleftarrows 2La_{Ba}^{\bullet} + 2Ti_{Ti}^{\prime} + 6O_O^{\times} + \frac{1}{2}O_2(g) \quad (1')$$

It was widely accepted that at higher donor dopant contents compensation occurs via an ionic mechanism with creation of cation vacancies, as Chan et al. reported earlier [16]. The nature of

* Corresponding author. Tel.: +40 232 201175; fax: +40 232 201205.
E-mail addresses: lavinia.curecheriu@uaic.ro (L.P. Curecheriu), lmtsr@uaic.ro (L. Mitoseriu).

0925-8388/$ – see front matter © 2011 Elsevier B.V. All rights reserved.
doi:10.1016/j.jallcom.2011.08.027

these cation vacancies was a long-term controversial topic. Thus, the model on La-doped $BaTiO_3$ of Daniels and Härdtl considered only the barium double-ionized vacancies as compensating ionic defects [14], as described by Eq. (2):

$$La_2O_3 + 3TiO_2 \rightleftarrows 2La_{Ba}^{\bullet} + 3Ti_{Ti}^{\times} + V_{Ba}'' + 9O_O^{\times}. \quad (2)$$

Jonker and Havinga, based on their XRD and TEM studies, showed that the type of the compensating cation vacancies strongly depends on both sintering conditions and nature of donor dopant [17]. In their variously donor-doped $BaTiO_3$ samples they found that ionic compensation can occur: (*i*) exclusively by titanium vacancies, according to the formula $Ba_{1-x}D_xTi_{1-x/4}O_3$ for (A-site donor doping) or $BaTi_{1-5x/4}D_xO_3$ (for B-site donor-doping, where D = donor) and (*ii*) by equal concentrations of barium and titanium vacancies, when some B-site donor doped $BaTiO_3$ compositions were sintered at different temperature than in the first case.

Later works based both on calculation of defect energy [18] and experimental evidences [15,16] revealed that titanium tetra-ionized vacancies are the most likely compensating defects in highly-donor doped $BaTiO_3$. More recently, Morisson et al. reported that the switch of ionic towards electronic charge compensation (involving the change in cation stoichiometry) induced by decreasing La content is unlikely to occur and that donor charge in La^{+3}-doped $BaTiO_3$ is always compensated only by Ti vacancies, while electrons are never the primary compensating defects, irrespective of the donor dopant content [19]. They sustained that n-type conductivity noticed even in reduced La-doped $BaTiO_3$ ceramics has to be rather associated with small amounts of oxygen loss during their sintering in air at temperature $\geq$1350 °C followed by quenching, according to the reaction (3) and this oxygen loss is not directly related to donor doping level [19–21].

$$O_O^{\times} \rightleftarrows \frac{1}{2}O_2 + V_O^{\bullet\bullet} + 2e' \quad (3)$$

Contrary to this view, in a reply in the same journal few months later, D.M. Smyth demonstrated that the observed reproducible and reversible weight loss on reduction, or gain on oxidation, is exactly that expected for a change between ionic and electronic compensation, corresponding to the loss or gain of the "excess" oxygen contained in the donor oxide, *e.g.* $LaO_{1.5}$ *vs.* the BaO it replaces [22]. He also showed by thermogravimetric analyses that the amount of this weight change is proportional to the donor concentration and the reversible switch from ionic to electronic compensation can be described by Eq. (4):

$$Ti_{Ti} + O_2 \rightleftarrows TiO_2 + V_{Ti}''' \quad (4)$$

where the TiO_2 excess would be expected to be expelled from the $BaTiO_3$ lattice as a $Ba_6Ti_{17}O_{40}$ secondary phase.

Consequently, depending on the amount and distribution of the defects (electrons, cation and oxygen vacancies) induced by the processing parameters (sintering temperature, sintering atmosphere and cooling rate), the resulted ceramic samples may be typical insulators, semiconductors, or alternatively, they may be even electrically heterogeneous showing giant values of the effective dielectric constant. It results that various types of applications exploiting either the semiconducting behaviour or the dielectric character might be tailored by a proper doping and/or sintering strategy. The most common dielectric properties reported in La-doped $BaTiO_3$ are the positive temperature coefficient of resistivity (PTCR) characteristics, characterised by a jump of a few order in magnitude of the resistivity in a small temperature range above the ferroelectric–paraelectric transition temperature [23]. Much less publications reported aspects concerning the dielectric behaviour in lightly La-doped compositions and none of them referred to the high field dielectric non-linear properties (tunability).

In the present paper the diffuse phase transition and dielectric tunability of La-doped $BaTiO_3$ (BLT) solid solutions prepared by the solid state reaction method was investigated. The observed dielectric non-linearity was described using Landau–Ginzburg–Devonshire (LGD) theory and its approach (Johnson [9] or even-power laws) for ceramics in ferroelectric state and by a multipolar mechanism model for ferroelectrics in their paraelectric state and for relaxors.

2. Sample preparation and experimental details

Ceramic samples with lower dopant content (x = 0.001; 0.0025; 0.005) corresponding to the $Ba_{1-x}La_xTiO_3$ formula (A/B ratio = 1, where A and B represents the species that occupy barium and titanium sites in ABO_3 perovskite lattice), as well as specimens with higher lanthanum proportion, having adjusted concentrations of built-in titanium vacancies ($A/B > 1$), of composition described by $Ba_{1-x}La_xTi_{1-x/4}O_3$ ($0.005 \leq x \leq 0.05$) formula, were prepared by the conventional ceramic method from p.a. grade oxides and carbonates: TiO_2 (Fluka), La_2O_3 (Merck) and $BaCO_3$ (Fluka), by a wet homogenization technique in iso-propanol. The initial mixtures were dried and shaped by uniaxial pressing at 160 MPa into pellets of 20 mm diameter and ~3 mm thickness. After the presintering thermal treatment performed in air at 1200 °C with 3 h plateau, the samples were finely ground in an agate mortar, pressed again into pellets (of 13 mm diameter and ~2 mm thickness) using an organic binder (5% solution of polyvinyl alcohol in water). These pellets were sintered in air at 1300 °C, with a heating rate of 5 °C/min and a soaking time of 6 h and then they were slowly cooled at the normal cooling rate of the furnace.

X-ray diffraction measurements at room temperature used to investigate the purity of the perovskite phases were performed with a *SHIMADZU XRD 6000* diffractometer using Ni-filtered CuKα radiation (λ = 1.5418 Å) with a scan step increment of 0.02° and with a counting time of 1 s/step, for 2θ ranged between 20° and 80°. To estimate the structural characteristics (unit cell parameters, tetragonality degree and unit cell volume), the same step increment but with a counting time of 10 s/step, for 2θ ranged between 20° and 120° was used. Parameters to define the position, magnitude and shape of the individual peaks were obtained using the pattern fitting and profile analysis of the original X-ray 5.0 program. The lattice constants calculation is based on the least squares procedure (LSP) using the linear multiple regressions for several XRD lines, depending on the unit cell symmetry.

A high resolution Quanta Inspect F, FEI Co. scanning electron microscope with field emission gun (FEG), coupled with EDX microprobe was used to analyze the microstructure and to check the chemical composition in the fracture of the ceramic samples.

For the lightly La-doped, stoichiometric ceramics (A/B = 1), thin foil specimens obtained by ion-beam milling (using a low angle ion milling and polishing system from Fischione) were examined by means of a transmission electron microscope Tecnai™ G^2 F30 S-TWIN equipped with energy-dispersive X-ray analyzer.

The sinterability of the BLT ceramics was estimated by means of the values of relative density calculated as percent ratio between the apparent density determined by the Archimedes method and the crystallographic (theoretical) density resulted from the diffraction data.

The electrical measurements were performed on parallel-plate capacitor configuration. Silver electrodes were applied on the polished surfaces of the sintered ceramic disks. The complex impedance in the frequency domain ($20–2 \times 10^6$) Hz and at temperatures of 20–200 °C was determined by using a Agilent E4980A Precision LCR Meat. For measuring the dc-tunability, the ceramic pellets were placed in a cell containing transformer oil. The tun-

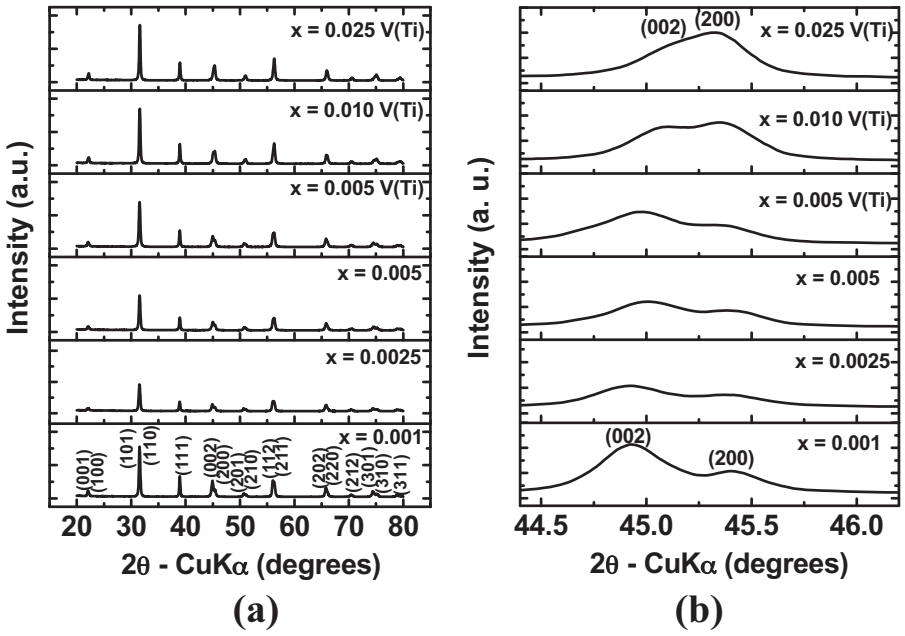

Fig. 1. (a) Room temperature X-ray diffraction patterns of La-doped barium titanate ceramics sintered in air at 1300 °C for 3 h; (b) (0 0 2)/(2 0 0) peak profiles indicating the structural evolution as a function of La content.

ability data were obtained using the circuit described in Ref. [24], in which high voltages up to ~50 kV/cm were obtained by a function dc-generator coupled with a TREK 30/20A-H-CE amplifier.

3. Results and discussions

For all the investigated ceramics resulted after sintering at 1300 °C/6 h, the room temperature XRD patterns (Fig. 1(a)) show the presence of single-phase perovskite compositions, in the limit of the XRD experiment accuracy. The lack of any Ba, Ti or La-rich secondary phases demonstrated that, in the mentioned sintering conditions, the solid state reactions, involving the incorporation of the La addition in the perovskite lattice, were completed.

If we assume the validity of the compensating mechanism by titanium vacancies also for the lightly La-doped solid solutions described by the $B_{1-x}La_xTiO_3$ formula, then titanium-rich secondary phases should be detected [15,16,19–21,25]. However, our XRD results seem to indicate that lower dopant amounts ($0.001 \leq x \leq 0.005$) can be accommodated in the perovskite lattice without segregation or precipitation of titanium-rich secondary phases, even if the compositions described by the formula $Ba_{1-x}La_xTiO_3$ have been designed to have no titanium vacancies as compensating defects. On the other hand, for the Ti vacancy-free samples, due to the very low dopant concentration, the presence of small amounts of some potential secondary phases found under the XRD detection limit cannot be excluded.

According to the phase diagram of the ternary $BaO–TiO_2–La_2O_3$ system at 1300 °C, proposed by Skapin et al. [26], even if a $BaTiO_3$ – $BaLa_2Ti_3O_{10}$ (BLT_3) tie line with extension to $La_2Ti_2O_7$ (LT_2) does not exist, the lightly La-doped $Ba_{1-x}La_xTiO_3$ compositions are placed in a domain of unique ternary solid solutions, adjacent to $BaTiO_3$. This means that, true single phase $Ba_{1-x}La_xTiO_3$ solid solutions can be formed for low La concentration, but in this case, other compensating mechanisms, *i.e.* electronic compensation or ionic compensation by equal number of double-ionized barium vacancies and tetra-ionized titanium vacancies have to be taken into account. Further SEM and/or TEM investigations coupled with EDX are required in order to try to detect the presence of small amounts of any secondary phases and electrical measurements, especially impedance spectroscopy, have to be carried out to determine the electric microstructure and, therefore, to elucidate the most likely compensating mechanisms for the supplementary positive charge induced by the donor center for lightly La-doped compositions described by the $Ba_{1-x}La_xTiO_3$ formula.

The change of the (0 0 2)/(2 0 0) peak profiles indicates the evolution of the unit cell symmetry with the increase of La content. For lower dopant concentrations ($x = 0.001$) an obvious splitting of the diffraction peak located at $2\theta = 44.5–45.5°$ emphasized a tetragonal structure, similar to those of pure $BaTiO_3$. The increase of lanthanum content, as well as the presence of titanium vacancies as compensating defects induced a gradual coalescence of (0 0 2) and (2 0 0) peaks, originating in the decrease of the tetragonality degree of the unit cell. For the ceramic with the highest lanthanum concentration ($x = 0.025$) analyzed here, instead of two clearly delimited peaks, only a broadened, asymmetric peak with a shoulder at its left side was identified. However, this asymmetry shows the persistence of a certain degree of tetragonality, suggesting that, at room temperature, the ceramic with the mentioned composition is still in its ferroelectric state (Fig. 1(b)). These results seem to be in agreement with those of West et al., who have reported that the tetragonal-cubic polymorphic change associated to the ferroelectric–paraelectric phase transition takes place at room temperature for a higher La content, *i.e.* $x = 0.05$ in $Ba_{1-x}La_xTi_{1-x/4}O_3$ solid solutions [25,27]. Indeed, the values of the structural parameters presented in Table 1 and calculated from the XRD data indicates, especially in the case of highly doped ceramics, a downward trend of the unit cell tetragonality expressed by the c/a ratio, as the La content increased. The increase of the dopant concentration, as well as the presence of the built-in titanium vacancies for the samples with higher La content also induced an expected shrinkage of the unit cell, taking into account the lower value of the ionic radius of La^{3+} (1.36 Å) in comparison with that one corresponding to the replaced Ba^{2+} ion (1.61 Å).

SEM investigations on the fracture of the sample with $x = 0.001$ emphasized a coarse and dense microstructure, similar to the undoped $BaTiO_3$, consisting predominantly of large grains, with non-uniform shape, but presenting well defined boundaries and triple junctions and an equivalent average size of ~63 μm

Table 1
Structural parameters and density of the investigated BLT ceramics sintered at 1300 °C for 6 h.

Sample	a (Å)	c (Å)	c/a	V (Å^3)	$\rho_{theortic}$ (g/cm^3)	$\rho_{apparent}$ (g/cm^3)	$\rho_{relative}$ (%)
$Ba_{0.999}La_{0.001}TiO_3$	3.9931(9)	4.0318(13)	1.0097(5)	64.28(5)	6.02	5.56	92.36
$Ba_{0.9975}La_{0.0025}TiO_3$	3.9934(11)	4.0330(16)	1.0099(7)	64.32(6)	6.02	5.42	90.03
$Ba_{0.995}La_{0.005}TiO_3$	3.9896(14)	4.0296(21)	1.0100(9)	64.14(8)	6.04	4.86	80.46
$Ba_{0.995}La_{0.005}Ti_{0.99875}O_3$	3.9903(14)	4.0278(20)	1.0093(9)	64.13(8)	6.03	5.24	86.90
$Ba_{0.99}La_{0.01}Ti_{0.9975}O_3$	3.9908(22)	4.0234(28)	1.0081(13)	64.08(12)	6.04	4.71	77.98
$Ba_{0.975}La_{0.025}Ti_{0.99375}O_3$	3.9896(19)	4.0156(30)	1.0065(12)	63.92(11)	6.05	4.48	74.05

(Fig. 2(a)). The wavy and rough surface profile of these grains (with bumps and hollows) shows that such a growth mechanism involved the increase of the larger grains at the expense of their smaller neighbours. This kind of grain morphology was noticed not only in $BaTiO_3$-based compositions but also in other perovskite systems as $CaCu_3Ti_4O_{12}$ [28]. A reduced amount of smaller grains (of ~5–9 μm) were still detected in the grain boundary or triple junction regions, as the higher magnification image of Fig. 2(b) pointed out (zone delimited by the white circle). SEM investigations in backscattered electron (BSE) mode, as well as EDX mapping and quantitative analyses performed on several such of small grains, on different grain boundary and triple junction regions of the larger grains indicated no evidence of secondary titanium or barium-rich secondary phases.

For the composition with $x = 0.0025$, the corresponding SEM image also shows a dense microstructure, but with a rather bimodal grain size distribution, indicating that as the La content increases, the amount of smaller grains becomes significant. Thus, larger grains (of 25–55 μm) coexist with smaller ones (of ~10 μm), as Fig. 2(c) pointed out.

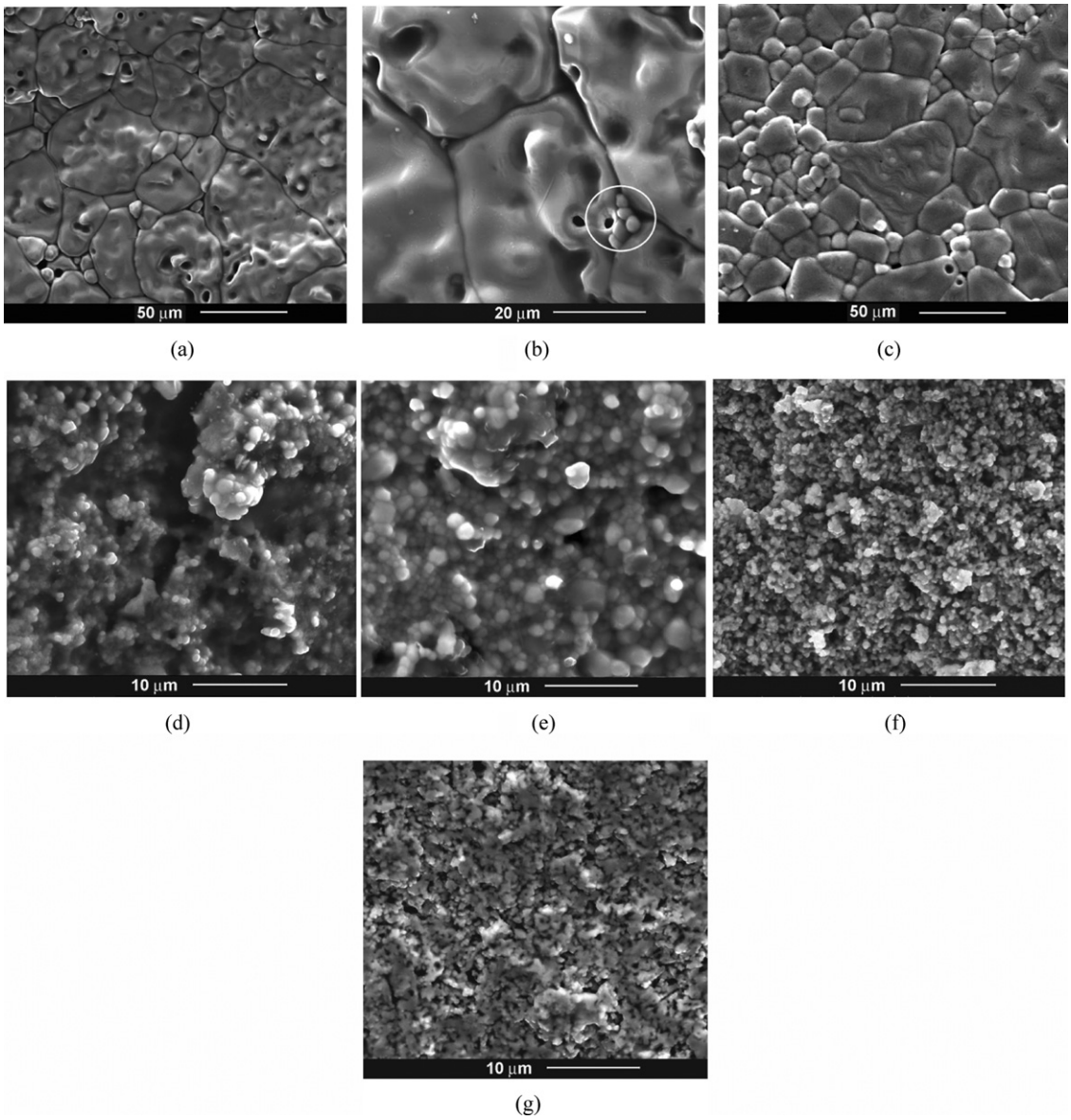

Fig. 2. SEM images in fracture of ceramic samples sintered in air at 1300 °C for 6 h: (a)–(d) $Ba_{1-x}La_xTiO_3$: (a) $x = 0.001$ – general view; (b) $x = 0.001$ – detail, (c) $x = 0.0025$ and (d) $x = 0.005$; (e)–(g) $Ba_{1-x}La_xTi_{1-x/4}O_3$: (e) $x = 0.005$; (f) $x = 0.01$ and (g) $x = 0.025$.

A dramatic microstructural change occurs for the samples with higher lanthanum content. The inhibiting effect of the donor dopant on the grain growth process becomes evident, so that for the composition with $x = 0.005$ a rather uniform microstructure, with an almost unimodal grain size distribution was observed, irrespective of the (Ba + La)/Ti ratio (Fig. 2(d) and (e)). Such a grain size decrease was earlier reported by Chan et al. in their Nb-doped $BaTiO_3$ ceramic with similar dopant content [16]. Despite the fact that the origin of the grain growth prevention for donor doping levels above a critical concentration in $BaTiO_3$ is a well-known phenomenon and has often been a subject of intensive investigation, a fully satisfying explanation has still not been obtained. Several approaches, including kinetic aspects [14], thermodynamic reasons [29], as well as grain boundary segregation phenomena [30] were proposed in order to elucidate this microstructural feature in heavily donor doped barium titanate ceramics. In our case, for a La content corresponding to $x = 0.005$, a slightly higher average grain size, a more regular spherical morphology and better delimited grain boundaries were noticed for grains corresponding to the composition with built-in titanium vacancies (Fig. 2(e)). From these observations we concluded that for similar La content, near the critical concentration, the presence of the built-in titanium vacancies seems to promote densification, inducing a certain decrease of the intergranular porosity. The cause of this behaviour remains still unclear. Average grain sizes of 1 μm and 1.5 μm were estimated for ceramic samples with $x = 0.005$, without and with built-in titanium vacancies, respectively.

The increase of the lanthanum concentration for ceramics with $x = 0.010$ and $x = 0.025$ leads to further microstructural disturbance by preventing grain growth and generating an increasing amount of intergranular porosity with negative effects on the densification (Fig. 2(e) and (f)). For both ceramic samples, homogeneous microstructures with unimodal grain size distributions, consisting of submicron grains (<600 nm) were observed (Fig. 2(f) and (g)).

The SEM observations are sustained by the relative density values presented in Table 1. The increase of the solute concentration induced a significant decrease of the relative density from ~92%, for the ceramic with $x = 0.001$, to ~74%, for the specimen corresponding to $x = 0.025$. In the case of the samples with the same La content ($x = 0.005$), but with different (Ba + La)/Ti ratio, a higher relative density of ~87% was estimated for the ceramic with built-in cation vacancies than that one (of ~80%) corresponding to the specimen without Ti vacancies.

TEM/EDS investigations carried out on thin foil specimens of lightly La-doped ceramics described by $Ba_{1-x}La_xTiO_3$ formula, did not reveal the presence of any Ti-rich secondary phase, even for the composition with the highest dopant content ($x = 0.005$).

The temperature dependence of the dielectric constant and tangent loss of the BLT ceramics with different concentration of La at a fixed frequency are presented in Fig. 3(a) and (b). The data revealed permittivity between 1000 and 2000 for all the compositions at room temperature. As reported by other authors for similar substitution degree, the Curie temperatures show a composition-induced shift of the ferroelectric-to-paraelectric phase transition [25]. By increasing the amount of La, the Curie temperature decreases from $T_C \sim 125\,^\circ C$ for $x = 0.001$ to $T_C \sim\,^\circ C$ for $x = 0.025$, together with a tendency towards a relaxor state characterised by a diffuse phase transition. A slightly steeper decrease of Curie temperature, of ~27 °C per at.% La, was obtained for the samples investigated here, in comparison with that of only 24 °C per at.% La reported by Morisson et al. [25]. For samples with $x = 0.005$, the cation stoichiometry expressed by (Ba + La)/Ti ratio has no influence on the temperature dependence of the dielectric constant and on the value of the Curie temperature (in both cases $T_C = 110\,^\circ C$). However, higher permittivity values were recorded in all the temperature range for the ceramic sample with Ti vacancies, suggesting that the donor dopant is easier accommodated and more effective in a $Ba_{1-x}La_xTi_{1-x/4}O_3$ solid solution than in the structure of the mixed crystals described by the $Ba_{1-x}La_xTiO_3$ formula. The dielectric loss of all the samples is below 12% in overall the investigated temperature range (Fig. 3(b)) and in particular, the tangent loss values were suppressed significantly at temperatures above T_C. The losses are smaller for the samples with a high La content and with built-in titanium vacancies V(Ti). In specimens with the same dopant concentration ($x = 0.005$) but with different (Ba + La)/Ti ratio, the evolution of the dielectric loss is also very similar. The higher values of dielectric losses recorded in the ceramic with titanium vacancies can be associated with the effectiveness of ferroelectric mechanism involving higher values of dielectric constant, as already mentioned. The increasing losses far above the Curie temperature (Fig. 3(b)) are related to thermally activated Maxwell–Wagner phenomena due to space charges present in the system.

The ferroelectric–paraelectric phase transition is sharper for ceramics with low La content and extends on a larger temperature range when increasing La amount, indicating a more diffuse character of the phase transition. For $x = 0.010$ and $x = 0.025$, a ferroelectric behaviour with diffuse phase transitions (DPT) is observed (Fig. 3(a)). The permittivity values for the ceramic with $x = 0.025$ sintered in air at 1300 °C/6 h are significantly lower for all the investigated temperatures, than those reported by Morisson et al. for the same composition but sintered at 1350 °C in flowing O_2 [21,25]. Besides, while in our case the ceramic with $x = 0.010$ already shows a diffuse phase transition, Morisson et al. reported this feature only for the composition with a significantly higher (of one order of

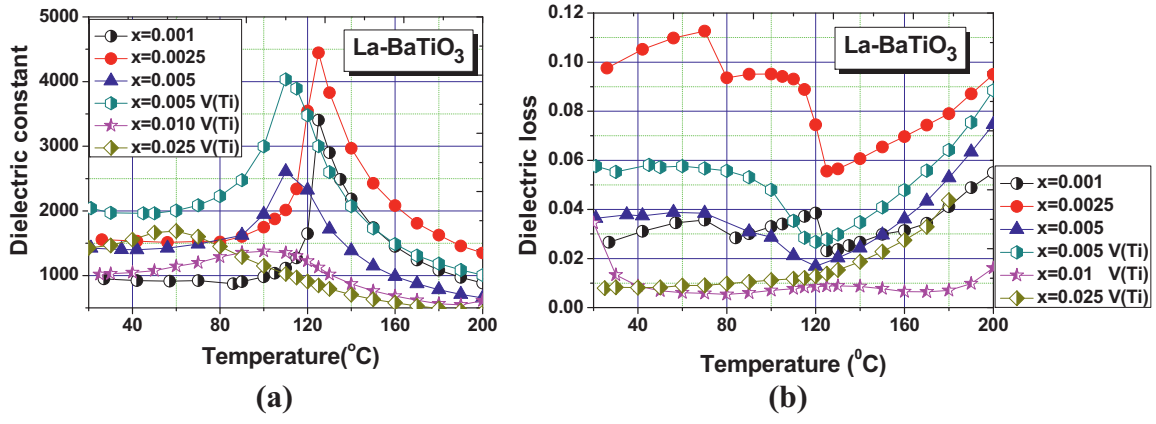

Fig. 3. Temperature dependence of (a) dielectric constant and (b) tangent loss for BLT ceramics at the frequency $f = 20$ kHz (the notationV(Ti) – indicates the presence of the "built-in" titanium vacancies in the BLT compositions).

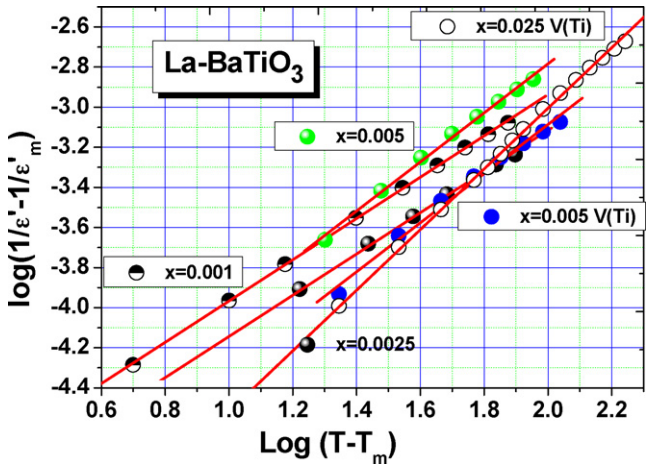

Fig. 4. Plot of the $\log((1/\varepsilon') - (1/\varepsilon'_m))$ as a function of $\log(T - T_m)$ for the dielectric data obtained at $f = 20$ kHz. The symbols are experimental data and the solid lines are fits with Eq. (2).

magnitude) La content, *i.e.* for $x = 0.10$. It is well known that diffuse phase transitions and ferroelectric–relaxor crossover is mainly common to *B*-site doping in $BaTiO_3$ [31]. However, many studies showed that microstructure can have also a significant influence from this point of view [32]. Thus, in very fine-grained $BaTiO_3$-based ceramics phase transition diffusiveness can be associated with distributed internal stress and local fields caused by small grain sizes. In our case, the increase in the phase transition diffusiveness can be related to this microstructural feature, as SEM images demonstrated.

For the full relaxor state with diffuse phase transition, a Vogel–Fulcher frequency dependence of the maximum permittivity temperature with frequency was commonly reported [33,34]. However, the very small frequency shift of the temperature corresponding to the permittivity maximum T_m with frequency does not allow to perform such a detailed analysis. In any case, it is clear that increasing La additions ($x = 0.01$ and $x = 0.025$), the relaxor–paraelectric transition takes place in a larger range of temperatures and not at a fixed Curie temperature T_C. In this temperature range, the maximum permittivity temperature T_m is also located. A modified Curie–Weiss law proposed by Uchino and Nomura [35] has been used to describe the diffuseness degree of the phase transition, as often used for other $BaTiO_3$-based solid solutions like BZT [36,37] or for Pb-based relaxors [38]:

$$\frac{1}{\varepsilon'} - \frac{1}{\varepsilon'_m} = \frac{(T - T_m)^\gamma}{C'} \quad (5)$$

where γ and C' are assumed to be constant. The parameter γ gives information on the character of the phase transition: for $\gamma = 1$, normal Curie–Weiss law is obtained while the value $\gamma = 2$ describes a complete diffuse phase transition. For a ferroelectric material, Eq. (5) reduces to the Curie–Weiss law, with $\gamma = 1$ and in this situation C' is proportional to the Curie constant. The plots of the $\log((1/\varepsilon') - (1/\varepsilon'_m))$ as function of $\log(T - T_m)$ for the investigated BLT samples are shown in Fig. 4. A linear relationship is found and the slope of the fitting curves (Eq. (5)) was used to determine the γ value. The results are presented in Table 2. The evolution towards the relaxor state with increasing x is demonstrated by the increase of the empirical parameter γ (which increases from 0.98 for $x = 0.0025$ to 1.52 for $x = 0.025$).

The dc-resistivity determined as a function of temperature (not shown here) present only PTCR anomaly above the corresponding Curie temperatures. However, the resistivity jump is below one order in magnitude (from $\sim 5 \times 10^3$–$10^4\ \Omega$ m at room temperature to maximum values in the range of $\sim 3 \times 10^4\ \Omega$ m above the Curie temperature). The small PTCR effect, the lack of giant values for the dielectric constant, the order of magnitude of the dielectric losses ($\sim 10^{-2}$) in the overall temperature range indicated in all these BLT compounds a typical dielectric behaviour and suggested no heterogeneous charge defect distribution in the ceramic grains (*e.g.* grain boundary phenomena originating the PTCR effect [23]). Detailed impedance spectroscopy analysis was carried out and confirmed this assumption. Fig. 5 shows the complex impedance characteristics for the BLT ceramics at room temperature. An apparent single component in impedance plots at room temperature (Fig. 5(a)), as well as for a higher temperature ($T = 200\ ^\circ$C – Fig. 5(b)) investigated here, illustrates a rather homogeneous defect distribution in ceramic samples, without any sign of a "brick-wall" electric microstructure, as Daniels et al. reported earlier for their La-doped ceramics [14]. While for single phase, non-stoichiometric ((Ba + La)/Ti ratio > 1) and highly La-doped ceramics with built-in titanium vacancies this result was expected, taking into account the occurrence of an undoubted ionic compensation mechanism of the donor dopant by means of Ti vacancies, as described by Eq. (6), the impedance data of stoichiometric ((Ba + La)/Ti ratio = 1), lightly doped specimens require a more careful analysis.

$$2La_2O_3 + 3TiO_2 \rightleftarrows 4La_{Ba}^{\bullet} + 3Ti_{Ti}^{\times} + V_{Ti}^{''''} + 12O_O^{\times} \quad (6)$$

It is well known that the ceramic microstructure plays also a significant role in the electrical behaviour of donor-doped $BaTiO_3$ [16]. From this point of view it was not surprising that, due to the normal furnace cooling, the small grains of the stoichiometric, lightly La-doped ceramic sample with $x = 0.005$ was fully oxidized, this explaining the single-component impedance plot. For stoichiometric, but coarse-grained ceramics ($x = 0.001$ and 0.0025, respectively), if electronic compensation at sintering temperature is assumed as prevailing mechanism, as Chan et al. sustained [16], then also a full oxidation caused by the slow cooling of these samples should take place to explain the single contribution in the impedance plots. However, such a complete oxidation, induced only by the furnace cooling rate, able to explain the homogeneous defect distribution in ceramic grains with sizes over 50–60 μm seems to be unlikely. If only a small region of grain core would have exhibited a semiconducting character due to electronic or mixed (electronic and ionic) compensation, then that would be clearly appeared as a second component in the corresponding impedance plots, beside the major grain boundary contribution. In other words, these large ceramic grains would have to be composed of an oxidized grain boundary depletion layer, whose thickness is directly related to the cooling rate and a semiconducting grain core, which in fact was not observed. Therefore, it is most likely to assume that even for these stoichiometric samples, the insulating behaviour mainly originates

Table 2
Temperature T_m corresponding to the maximum dielectric constant ε_m, diffuseness constant γ (computed from data at 20 kHz) and tunability n, for the BLT samples.

Samples	$x = 0.001$	$x = 0.0025$	$x = 0.005$	$x = 0.005$ V(Ti)	$x = 0.010$ V(Ti)	$x = 0.025$ V(Ti)
T_m (°C)	125	125	110	110	100	60
ε_m	3405	4446	2608	4033	1374	1689
γ	1.03	0.98	1.15	1.23	1.98	1.52
n	1.14	–	1.51	1.44	1.19	1.57

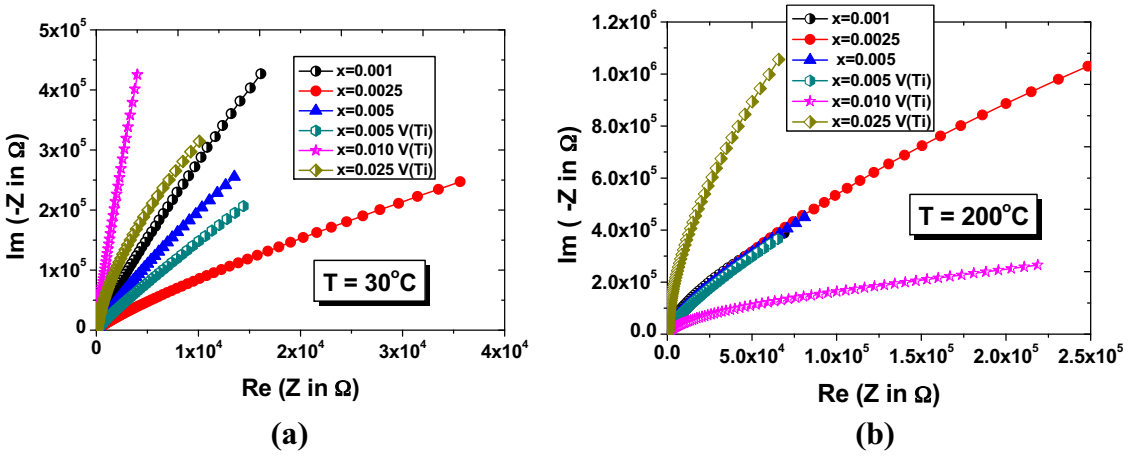

Fig. 5. Complex impedance plots for BLT ceramics at two extreme temperature: (a) 30 °C and (b) 200 °C.

in a predominant ionic compensation of the donor dopant at the sintering temperature. These results seem to disagree with those reported by Chan et al. [16] regarding Nb-doped $BaTiO_3$ ceramics, also sintered in air and cooled at the normal furnace rate. Thus, while their dark-coloured $BaTi_{0.9975}Nb_{0.0025}O_3$ ceramic exhibited semiconducting behaviour which was explained in terms of a predominantly electronic compensation of the supplementary positive charge of niobium, our yellowish $Ba_{0.9975}La_{0.0025}TiO_3$ composition is a typical insulator, with homogeneous defect distribution, where compensation of La by ionic defects seems to prevail. This apparent contradiction is overcome if the different sintering temperature is taken into account. Thereby, the Nb-doped sample of Chan et al. was sintered at a significant higher temperature, *i.e.* 1450 °C than our La-doped ceramic with similar composition (1300 °C). From this point of view, it is worthy to mention that a higher sintering temperature favours the electronic compensation by extending the region where $n = [D^{\bullet}]$ in the $\log\sigma - \log P_{O_2}$ plot towards higher oxygen activities, as Smyth showed in his excellent report [22]. Consequently, because of the high sintering temperature, for the Nb-doped ceramic the furnace cooling will be not longer effective in a full oxidation, so that in the grain core region the high-temperature defect structure (*i.e.* predominantly electrons) is frozen, resulting in a semiconducting behaviour. In our case, the sintering temperature, of only 1300 °C, is more favourable for an ionic compensation and the influence of furnace heating is an additional contribution to the observed insulating behaviour. The results of Daniels et al. sustained this assertion, showing that for sintering in air, at lower temperatures (1220–1250 °C), a stoichiometric composition with a close donor dopant content, *i.e.* $BaTiO_3$ doped with 0.3 at.% La ($x = 0.003$), was insulating even after rapid cooling (quenching from the sintering temperature) [14]. Their $\log\sigma - \log P_{O_2}$ plot for several La-doped ceramics, presented also by Smyth [22], indicated that, for lower La amounts (0.1–0.3 at.% La) at an oxygen activity of 0.2 atm. ($\log P_{O_2} \sim -0.7$) corresponding to sintering in air, these compositions are found close to the region of the intrinsic minimum conductivity, where de extra-charge of the donor dopant is balanced by ionic defects with negative effective charge (*i.e.* cation vacancies). These earlier evidences are in accord with our impedance data and sustain the assumption of the lack of any grain bulk electronic compensation mechanism, including in the ceramics described by $Ba_{1-x}La_xTiO_3$ formula, when they are sintered in air at lower sintering temperatures and slowly cooled. This means that not always a coarse-grained microstructure of stoichiometric, lightly donor-doped $BaTiO_3$ ceramic is related with conducting properties.

Another problem which has to be solved is the type of the compensating defects which maintain the electric balance in stoichiometric, lightly La-doped ($x \leq 0.005$) samples. If we assume a real single phase composition for these ceramics, as XRD and SEM–TEM/EDS investigations revealed, then for a prevailing ionic compensation, two mechanisms of charge balance should be considered:

(a) Creation of interstitial anions, according to Eq. (7):

$$La_2O_3 + 2TiO_2 \rightleftarrows 2La_{Ba}^{\bullet} + 2Ti_{Ti}^{\times} + 6O_O^{\times} + O_i'' \quad (7)$$

(b) Creation of equal number of barium and titanium vacancies, as described by Eq. (8):

$$3La_2O_3 + 6TiO_2 \rightleftarrows 6La_{Ba}^{\bullet} + 6Ti_{Ti} + V_{Ba}'' + V_{Ti}'''' + 21O_O^{\times} \quad (8)$$

For energetic reasons, the formation of anti-Schottky defects (described by Eq. (7)) consisting of oxygen ions placed on interstitial sites is unlikely in the close-packed perovskite lattice of $BaTiO_3$ [18]. Consequently, it seems that the most plausible compensating mechanism should be that one consisting in creation of both barium and titanium vacancies, described by Eq. (6). However, for so low values of lanthanum concentration, when the single phase composition is uncertain because of the limits of the investigation methods and equipments, it is very hard to exactly identify the type of cation vacancy generated to maintain the electrical neutrality in donor doped $BaTiO_3$ ceramics. Chan et al. showed that even in their barium-deficient, but highly Nb-doped ceramic ($Ba_{0.97}Ti_{0.94}Nb_{0.06}O_{3.15}$), compensation occurred by titanium vacancies. Morisson et al. sustained the exclusive Ti vacancy compensation, also for fully oxidized, stoichiometric $Ba_{1-x}La_xTiO_3$ ceramics, regardless of x value, even if for low donor dopant concentrations they did not detected a titanium-rich secondary phase [21]. On the other hand, the creation of equal concentrations of barium and titanium vacancies seems to be actually not so unlikely. Our results indicated that the perovskite lattice is able to accommodate low lanthanum concentrations, without expelling the "extra" titanium (in order to adjust the A/B ratio), as the compensating mechanism which involves the exclusive creation of titanium vacancies requires. Compensating mechanism by equal number of barium and titanium vacancies was found not only in the earlier study of Jonker and Havinga concerning defect structure and phase relations in some donor-doped $BaTiO_3$ systems [17], but more recently, it was reported also by Wand and Sakka in some La-doped $Sr_{1-x}Ba_xTiO_3$ solid solutions [39] and was also found to contribute to the compensation of $OH^{\bullet}$ defects in hydrothermally prepared,

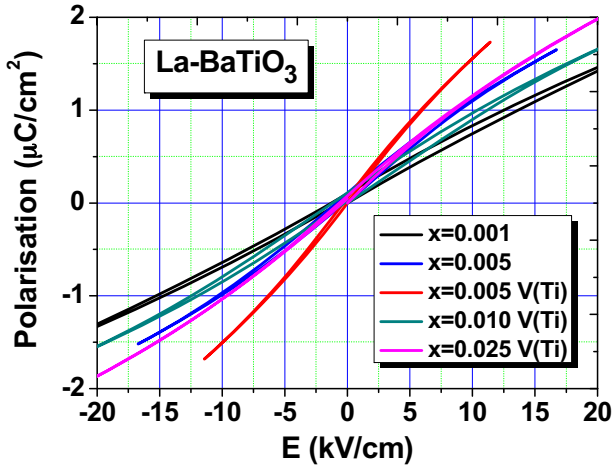

Fig. 6. Hysteresis loop for BLT ceramics at room temperature.

undoped $BaTiO_3$ powders [40]. Therefore, one can conclude that a mixed ionic compensation, implying the coexistence of Ba and Ti-site cation vacancies cannot be a priori excluded. Concerning the ceramics with similar lanthanum content ($x = 0.005$), but with different A/B ratio, taking into account that both are single-phase, it results that the ionic compensating mechanism at sintering temperature in air is quite different (*i.e.* by titanium vacancies for the non-stoichiometric sample, where $[La^{\bullet}] = 4[V'''_{Ti}]$ and by mixed barium and titanium vacancies for the stoichiometric one, where $[La^{\bullet}] = 2[V''_{Ba}] + 4[V'''_{Ti}]$), indicating that the type of the compensating defects could depend on the place of the compositions in the ternary $BaO–TiO_2–La_2O_3$ phase diagram.

The ferroelectric and non-linear dielectric properties were further determined. The polarization-field $P(E)$ hysteresis loops under quasi-static fields were recorded at room temperature and the results are shown in Fig. 6. The composition $x = 0.0025$ was subjected to a dielectric breakdown before being characterised from the point of view of tunability and $P(E)$ characteristics. All the other compositions presented well reproducible high-field responses, which are presented in the following.

As expected, due to the tendency towards the relaxor behaviour, the hysteretic nature of the $P(E)$ curve tends to strongly reduce by comparison with the reported $P(E)$ loops in pure $BaTiO_3$ ceramics [1], when La is added. All the compositions show $P(E)$ loops with very small area and remanent polarization and with coercivities in the range of 0.16–0.58 kV/cm. Irrespective of composition and compensation mechanism, the loops are rather tilted and unsaturated as results of both compositional and microstructural effects (very fine submicron grains for higher La addition). Similar loops are typical for Pb-based relaxors [[33] and Refs. herein] and for fine submicron grained $BaTiO_3$ ceramics [41]. For comparison, the field-induced polarization at a field of 10 kV/cm are in the range of 0.75–1.53 μC/cm^2, the highest corresponding to the composition $x = 0.005$ V(Ti) and the smallest to $x = 0.001$ (Fig. 6). A more detailed comparative analysis of the composition influence on the $P(E)$ loops characteristics is not possible, due to the non-saturation of the loops. In any case, we find that all the BLT ceramics shows a rather weak hysteretic character, although its non-linear character is undoubted. Non-linear dielectric properties and lack of hysteretic behaviour are desirable features for tunability applications.

The permittivity-field $\varepsilon(E)$ dependence (dc-tunability) was measured at room temperature. The data corresponding to all the investigated compositions are shown in Fig. 7(a). A non-linearity is observed for all the compositions, with a tendency towards saturation for very high fields only (~20 kV/cm), particularly for the samples with Ti vacancies with compositions $x = 0.005$ and $x = 0.025$. After the first dc-field cycles, the non-linear field-dependence $\varepsilon(E)$ tends to stabilize and the tunability data are well reproducible for all the investigated ceramic samples (non-hysteretic behaviour). For a given value of the applied field $E = 15$ kV/cm, the largest tunability $n = \varepsilon(0)/\varepsilon(E)$ was obtained for the composition $x = 0.005$ with built-in titanium vacancies ($n = 1.51$), while the sample with a reduced La content ($x = 0.001$) presents the lowest tunability ($n \sim 1.14$). The compositions $x = 0.001$ and $x = 0.01$ V(Ti) meet the requirement of permittivities below ~1000 for possible tunability applications, but their tunability is rather low at reasonable fields and only above 20 kV/cm the tunability of sample with $x = 0.01$ V(Ti) reaches values higher than $n = 1.4$. This composition is a kind of optimum for tunability applications in the investigated series of BLT compositions.

By analyzing the permittivity response in the low field region (below $\sim 5 \times 10^5$ kV/cm) it can be observed that the dielectric constant of the ceramics with smaller La content has the lowest field variation and the dc-tunability slightly increases with La content (Fig. 7(b)). This behaviour can be explained by taking into account that pure $BaTiO_3$ has mainly 180° domains and a very small amount of La would not produce a large modification in its permittivity [42]. Larger addition of La favours the 90° domain walls formation. Such domain walls are easier re-orientable by low fields and they give a response with a strong variation of the field-induced permit-

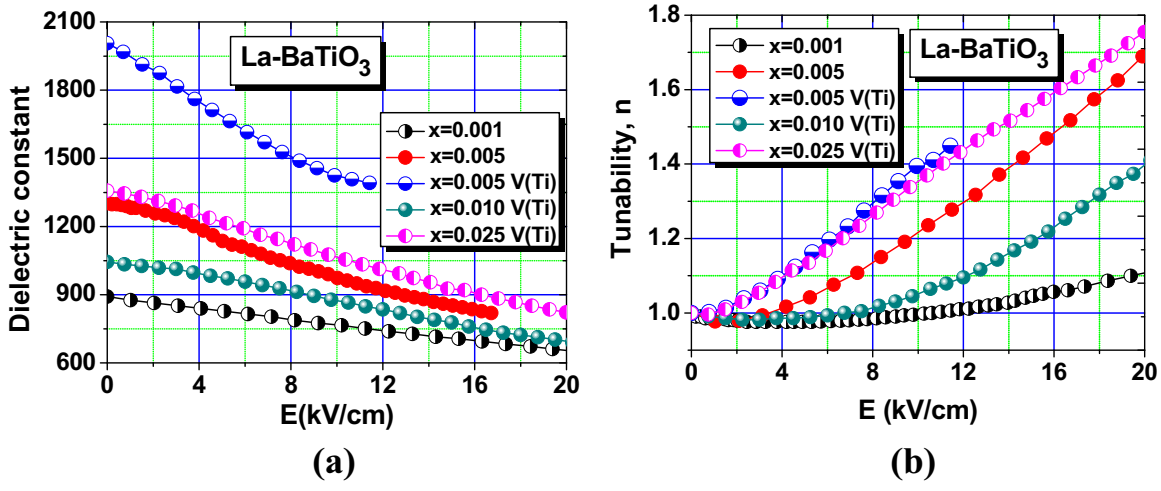

Fig. 7. (a) Dielectric constant *vs.* applied electric field at room temperature for the BLT ceramics; (b) Tunability $n = \varepsilon(0)/\varepsilon(E)$ *vs.* applied electric field for BLT ceramics.

tivity [8]. By the combined effect of La addition with Ti vacancies compensation, the tunability increases and shows an optimum for the composition $x = 0.005$ V(Ti). The largest tunability values for the concentrations $x = 0.005$ and 0.025 can be correlated with the proximity of their permittivity peak, as seen in Fig. 3.

In order to better understand the different mechanisms that contribute to the non-linear dielectric properties, it has to be taken into account that permittivity in perovskite ferroelectrics is the result of multiple polarization mechanisms whose behaviour under electric field sequence is rather difficult to be interpreted. The observation that tunability of ferroelectrics is higher in the relaxor state demonstrated that there is not a direct relationship between high spontaneous polarization, high permittivity and high tunability [2]. Although the domain walls in the ferroelectric state give an extrinsic contribution to the permittivity, their role in tunability is not essential. This is demonstrated by the fact that ferroelectrics in their paraelectric state and relaxors commonly present a high tunability. Instead, field-induced dipole reorientations or field-induced transformation of non-ferroelectric regions into ferroelectric ones seem to be at the origin of high tunability. Diamond [8] proposed in the sixties a model to explain the contributions to the tunability. According to this approach, a system with widely distributed Curie temperatures containing a mixture of ferroelectric and paraelectric regions in the Curie range will result in a high tunability, due to the fact that a field-induced transformation of the paraelectric into ferroelectric state is achieved at local scale. By increasing the diffuseness of phase transition in a ferroelectric, it can be obtained more regions which might be subjected to such a transformation. The dc-tunability data of such a ferroelectric system can be explained considering a complete model that takes into account the intrinsic ferroelectric polarization contribution, as well as extrinsic mechanisms that occur from cluster polarization, normally active at moderate fields [43]. This additional contribution to the polarization is due to the polar (but non-ferroelectric) nanodomains which are re-orientable by the applied field. The presence of such polarizable regions is commonly described by completing the Johnson's equation [9] with a Langevin term, which is dependent on the nanodomains' volume and polarization and on the temperature, according to the relation:

$$\varepsilon_r = \frac{\varepsilon_r(0)}{\{1 + \lambda[\varepsilon_0\varepsilon_r(0)]^3E^2\}^{1/3}} + \frac{P_0 x}{\varepsilon_0}[\cosh(Ex)]^{-2}, \quad x = P_0V/k_BT \quad (9)$$

where P_0 is the polarization of a nanodomain, V is its volume, k_B the Boltzmann constant and T is the temperature [39]. Using Eq. (9), the dc-tunability data of the present BLT ceramics with compositions $x = 0.005$, 0.01 and 0.025 were well fitted (with a statistical correlation of 0.998), as shown in Fig. 8(a–d).

The different contributions to the dc-tunability were estimated as following: at low fields (up to ~5 kV/cm), the extrinsic contribution is important and it may be correlated with the orientation degree of the polar nanoregions, while at moderate and high fields the dielectric non-linearity can be described again with the Johnson model and is mainly related to the field-induced ferroelectric polarization response. The highest contribution to the dielectric constant given by extrinsic mechanisms (of about ~10%) was obtained for the samples with $x = 0.005$. For higher amounts of La the charge compensation by titanium vacancies became predominant and the dielectric non-linearity comes from the ferroelectric response only. The samples with $x = 0.005$ La content seem to present an optimum

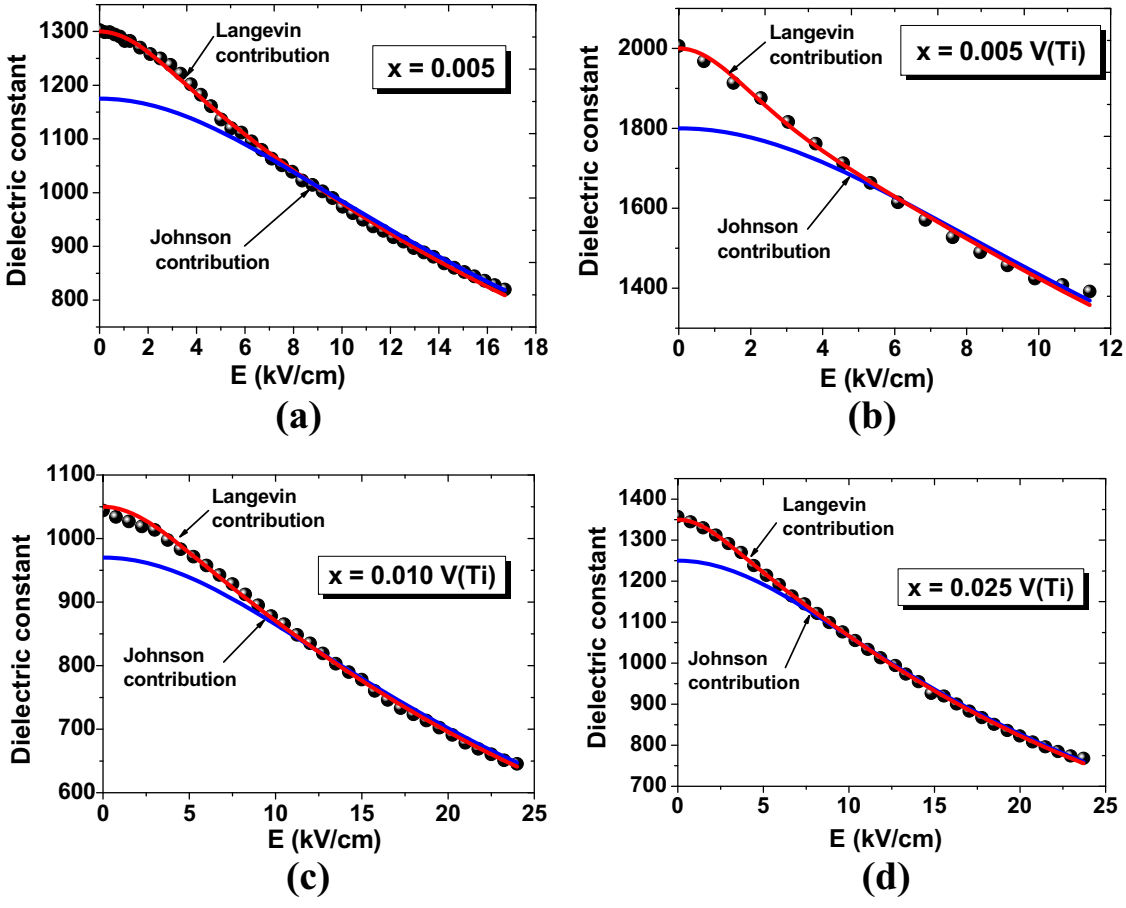

Fig. 8. Tunability data for BLT ceramics with various compositions and fits with multipolar mechanism model (Eq. (6)).

combination between composition (that gives extrinsic contribution) and grain size (knowing that an average grain size around 1 μm gives the largest number of 90° domain walls, thus inducing a larger intrinsic contribution to ferroelectric part of non-linearity). In any case, the reduced dielectric constant ($\varepsilon \sim 2000$), low losses at zero field ($\tan\delta < 6\%$) and tunability around 1.5 make from BLT ceramics promising candidate for tunable applications.

4. Conclusions

La-doped $BaTiO_3$ ceramics with different stoichiometry and lanthanum contents ($x = 0.001$; 0.0025; 0.005; 0.01 and 0.025) were prepared by a solid state reaction method and sintered at 1300 °C for 6 h. The phase purity and microstructural characteristics were investigated. All the compositions are single phase perovskites, with a tendency of transition from tetragonal to cubic when increasing the La addition. The dielectric properties were studied as function of temperature and frequency. With the increasing of La content, the Curie temperature of BLT ceramics decreases and the diffuse phase transition became obvious. All the ceramics under investigations were insulators with homogeneous defect distribution, as the impedance data revealed. The non-linear properties and tunability of the ceramic samples were reported for the first time. As the La addition increases, the $\varepsilon(E)$ dependence tends to reduce its hysteresis, thus transforming into a non-hysteretic relaxor. The dc-non-linear behaviour was analyzed using a multipolar mechanism model able to explain the higher tunability values in terms of other additional polarization mechanisms, as described by considering Langevin contribution to the $\varepsilon(E)$ dependence.

Acknowledgement

The financial support of the POSDRU 107/1.5/S/78342 grant under the RAMTECH center (162/15.06.2010 of POS CCE – A2-O2.1.2) is highly acknowledged.

References

[1] M.E. Lines, A.M. Glass, Principles and Applications of Ferroelectrics and Related Materials, Clarendon Press, Oxford, 1977.
[2] A.K. Tagantsev, V.O. Sherman, K.F. Astafiev, J. Venskatesh, N. Setter, J. Electroceram. 11 (2003) 5.
[3] R.E. Treece, J.B. Thompson, C.H. Mueller, T. Rivkin, M.W. Cromar, IEEE Trans. Appl. Supercond. 7 (2) (1997) 2363.
[4] Y. Somiya, A.S. Bhalla, L. Eric Cross, Inter. J. Inorg. Mater. 3 (2001) 709.
[5] W. Kleemann, J. Dec, R.P. Wang, M. Itoh, Phys. Rev. B 67 (2003) 092107.
[6] L.P. Curecheriu, A. Ianculescu, L. Mitoseriu, J. Alloys Compd. 482 (2009) 1–4.
[7] M.W. Cole, W.D. Nothwang, C. Hubbard, E. Ngo, M. Ervin, J. Appl. Phys. 93 (11) (2003) 9218.
[8] H. Diamond, J. Appl. Phys. 32 (1961) 909.
[9] K.M. Johnson, J. Appl. Phys. 33 (1962) 2826.
[10] C.E. Ciomaga, M. Viviani, M.T. Buscaglia, V. Buscaglia, L. Mitoseriu, A. Stancu, P. Nanni, J. Eur. Ceram. Soc. 27 (2007) 4061.
[11] G.H. Jonker, Solid-State Electron. 7 (1964) 895.
[12] O. Saburi, J. Phys. Soc. Jpn. 14 (1959) 1159.
[13] V.J. Tennery, R.L. Cook, J. Am. Ceram. Soc. 44 (1961) 187.
[14] J. Daniels, K.H. Hardtl, D. Hennings, R. Wernicke, Philips Res. Rep. 31 (1976) 487.
[15] M.H. Chan, D.M. Smyth, J. Am. Ceram. Soc. 67 (1984) 285.
[16] M.H. Chan, M.P. Harmer, D.M. Smyth, J. Am. Ceram. Soc. 69 (1986) 507.
[17] G.H. Jonker, E.E. Havinga, Mater. Res. Bull. 17 (1982) 345.
[18] C.V. Lewis, C.R.A. Catlow, J. Phys. Chem. Solids 47 (1986) 89–97.
[19] F.D. Morrison, D.C. Sinclair, J.M.S. Skakle, A.R. West, J. Am. Ceram. Soc. 81 (1998) 1957.
[20] F.D. Morrison, D.C. Sinclair, A.R. West, J. Am. Ceram. Soc. 84 (2001) 474.
[21] F.D. Morrison, A.M. Coats, D.C. Sinclair, A.R. West, J. Electroceram. 6 (2001) 219–232.
[22] D.M. Smyth, J. Elecroceram. 9 (2002) 179.
[23] J. Nowotny, M. Rekas, Ceram. Int. 17 (1991) 227.
[24] F.M. Tufescu, L. Curecheriu, A. Ianculescu, C.E. Ciomaga, L. Mitoseriu, J. Optoelectron. Adv. Mater. 10 (2008) 1894.
[25] F.D. Morrison, D.C. Sinclair, A.R. West, J. Appl. Phys. 86 (11) (1999) 6355.
[26] S.D. Skapin, D. Kolar, D. Suvorov, Z. Samardzija, J. Mater. Res. 13 (1998) 1327–1334.
[27] A.R. West, T.B. Adams, F.D. Morrison, D.C. Sinclair, J. Eur. Ceram. Soc. 24 (2004) 1439–1448.
[28] T.T. Fang, H.K. Shiau, J. Am. Ceram. Soc. 87 (2004) 2072–2079.
[29] M. Drofenik, Acta Chim. Slov. 46 (1999) 355–364.
[30] S.B. Desu, S.A. Payne, J. Am. Ceram. Soc. 73 (1990) 3407–3415.
[31] X.G. Tang, K.H. Chew, H.L.W. Chan, Acta Mater. 52 (2004) 5177–5183.
[32] C.E. Ciomaga, M.T. Buscaglia, M. Viviani, V. Buscaglia, L. Mitoseriu, A. Stancu, P. Nanni, Phase Trans. 79 (6–7) (2006) 389–397.
[33] Z.G. Ye, Key Eng. Mater. 81 (1998) 155–156.
[34] R. Pirc, R. Blinc, Phys. Rev. B 76 (2007) 020101(R).
[35] K. Uchino, S. Nomura, Ferroelectr. Lett. Sect. (1982) 44–55.
[36] C. Ciomaga, M. Viviani, M.T. Buscaglia, V. Buscaglia, L. Mitoseriu, A. Stancu, P. Nanni, J. Eur. Ceram. Soc. 27 (2007) 4061–4064.
[37] D. Ricinschi, C.E. Ciomaga, L. Mitoseriu, V. Buscaglia, M. Okuyama, J. Eur. Ceram. Soc. 30 (2010) 237–241.
[38] L. Mitoseriu, A. Stancu, C. Fedor, P.M. Vilarinho, J. Appl. Phys. 94 (2003) 1918.
[39] L. Wand, Y. Sakka, J. Am. Ceram. Soc. 93 (2010) 2903–2908.
[40] D.F.K. Hennings, C. Metzmacher, B.S. Schreinemacher, J. Am. Ceram. Soc. 84 (2001) 179–182.
[41] M.T. Buscaglia, M. Viviani, V. Buscaglia, L. Mitoseriu, A. Testino, P. Nanni, Z. Zhao, M. Nygren, C. Harnagea, D. Piazza, C. Galassi, Phys. Rev. B 73 (2006) 064114.
[42] J.E. Burke, R.C. DeVries, J. Am. Ceram. Soc. 40 (1957) 200.
[43] C. Ang, Z. Yu, Phys. Rev. B 69 (2004) 174109.